

Electron doping in FeSe monolayer and multilayer via metal phthalocyanine adsorption: A first-principles investigation

Fangyu Yang(杨方玉), Yan-Fang Zhang(张艳芳), Peixuan Li(李佩璇), and Shixuan Du(杜世萱)
Citation: Chin. Phys. B, 2025, 34 (**11**): 117302. DOI: 10.1088/1674-1056/ae0396
http://cpb.iphy.ac.cn; http://iopscience.iop.org/cpb

What follows is a list of articles you may be interested in

Freestanding $La_2CuO_4/La_{1.55}Sr_{0.45}CuO_4$ heterostructure membranes with high-T_c interface superconductivity

Xueshan Cao(曹雪珊), Chuanyu Shi(史传宇), Yanzhi Wang(王彦智), Meng Zhang(张蒙), Jirong Sun(孙继荣), and Yanwu Xie(谢燕武)
Chin. Phys. B, 2025, 34 (**10**): 107301. DOI: 10.1088/1674-1056/adf4a3

Role of self-assembled molecules' anchoring groups for surface defect passivation and dipole modulation in inverted perovskite solar cells

Xiaoyu Wang(王啸宇), Muhammad Faizan, Kun Zhou(周琨), Xinjiang Wang(王新江), Yuhao Fu(付钰豪), and Lijun Zhang(张立军)
Chin. Phys. B, 2024, 33 (**10**): 107303. DOI: 10.1088/1674-1056/ad711f

Improving the electrical performances of InSe transistors by interface engineering

Tianjun Cao(曹天俊), Song Hao(郝松), Chenchen Wu(吴晨晨), Chen Pan(潘晨), Yudi Dai(戴玉頓), Bin Cheng(程斌), Shi-Jun Liang(梁世军), and Feng Miao(缪峰)
Chin. Phys. B, 2024, 33 (**4**): 047302. DOI: 10.1088/1674-1056/ad24d7

Superconductivity in epitaxially grown $LaVO_3/KTaO_3(111)$ heterostructures

Yuan Liu(刘源), Zhongran Liu(刘中然), Meng Zhang(张蒙), Yanqiu Sun(孙艳秋), He Tian(田鹤), and Yanwu Xie(谢燕武)
Chin. Phys. B, 2023, 32 (**3**): 037305. DOI: 10.1088/1674-1056/acac1b

Bias-induced reconstruction of hybrid interface states in magnetic molecular junctions

Ling-Mei Zhang(张令梅), Yuan-Yuan Miao(苗圆圆), Zhi-Peng Cao(曹智鹏), Shuai Qiu(邱帅), Guang-Ping Zhang(张广平), Jun-Feng Ren(任俊峰), Chuan-Kui Wang(王传奎), and Gui-Chao Hu(胡贵超)
Chin. Phys. B, 2022, 31 (**5**): 057303. DOI: 10.1088/1674-1056/ac3caf

---

RAPID COMMUNICATION

Electron doping in FeSe monolayer and multilayer via metal phthalocyanine adsorption: A first-principles investigation

Fangyu Yang(杨方玉)[1,2], Yan-Fang Zhang(张艳芳)[1,2], Peixuan Li(李佩璇)[1,2], and Shixuan Du(杜世萱)[1,2,3,†]

[1] *Beijing National Laboratory for Condensed Matter Physics and Institute of Physics, Chinese Academy of Sciences, Beijing* 100190, *China*
[2] *School of Physical Sciences, University of Chinese Academy of Sciences, Beijing* 100190, *China*
[3] *Songshan Lake Material Laboratory, Dongguan* 523808, *China*

(Received 16 June 2025; revised manuscript received 20 August 2025; accepted manuscript online 5 September 2025)

Electron doping has been established as an effective method to enhance the superconducting transition temperature and superconducting energy gap of FeSe thin films on strontium titanate ($SrTiO_3$) substrates. Previous studies have demonstrated that electron/hole doping can be achieved through the adsorption of metal phthalocyanine (*M*Pc, M = Co, Cu, Mn, Fe, and Ni) molecules on surfaces. This work explores the electron doping induced by the adsorption of MPc molecules, specifically cobalt phthalocyanine (CoPc) and copper phthalocyanine (CuPc), onto FeSe monolayer and multilayers. Utilizing first-principles calculations based on density functional theory, we demonstrate that charge rearrangement occurs when MPc molecules adsorb on the FeSe substrate, contributing to an accumulation of electrons at the interface. In the CoPc/FeSe systems, the electron accumulation increases with the layer number of FeSe substrate, converging for substrates with 3–5 layers. The analysis of the integrated planar charge difference up to the position with zero integrated charge transfer reveals that all the five MPc molecules donate electrons to the uppermost FeSe layer. The electron donation suggests that MPc adsorption can be a promising strategy to modulate the superconductivity of FeSe layers.

Keywords: metal-phthalocyanine, multilayer FeSe, electron doping, interfaces

PACS: 73.20.–r, 68.35.–p, 73.40.–c, 98.38.Am

DOI: 10.1088/1674-1056/ae0396 **CSTR:** 32038.14.CPB.ae0396

1. Introduction

The discovery of high-temperature superconductivity (HTSC) in iron-based materials, particularly in iron selenide (FeSe) grown epitaxially on oxide substrates to nanoscale thickness,[1] has sparked significant scientific interest.[2] Observations have revealed significant increases in the critical temperature of monolayer FeSe when grown on $SrTiO_3$ substrates, achieving transition temperatures up to 100 K.[3] Despite considerable interest, the precise mechanisms underpinning HTSC in monolayer FeSe on STO substrates remain a mystery. Previous experiments have indicated that electron doping[4–6] and interface-enhanced electron–phonon coupling[7–9] are two key factors for the observed high-temperature superconductivity in the FeSe/STO system. Direct imaging of charge transfer at FeSe/$SrTiO_3$ interface has been observed in experiments,[10] which was also evidenced by intense electron doping within the FeSe monolayer.[11–13] Additionally, the absence of superconductivity in bilayer and thicker FeSe variants[14,15] highlights the critical role of doping levels in triggering superconductivity in these thicker films.

Organic molecule adsorption has demonstrated its potential in enhancing the superconducting properties through precise electron concentration control due to the interface-induced charge transfer and electron–phonon coupling.[16,17] These organic molecules also offer advantages in terms of stability and precision over traditional metal atom deposition methods such as potassium,[18,19] facilitating the self-assembly of well-ordered monolayers through van der Waals interactions. Metal phthalocyanine (MPc) molecules have been employed to tune the superconducting state and T_c of some superconductors.[19,20] For instance, the T_c of the atomic-layer superconductor, Si(111)-($\sqrt{7}\times\sqrt{3}$)-In, has been increased up to 4%[16] attributed to hole doping induced by CuPc adsorption.[20] Conversely, when manganese phthalocyanine (MnPc) is adsorbed on the surface, T_c decreases and the superconductivity is eventually suppressed. A slight reduction in T_c has been observed in iron phthalocyanine (FePc) thin film on a Si(111)-($\sqrt{7}\times\sqrt{3}$)-In heterostructure. This contrasts sharply with the strong suppression observed in the MnPc/Si(111)-($\sqrt{7}\times\sqrt{3}$)-In system, despite both heterostructures exhibiting similar magnetic properties and molecule–substrate charge transfer characteristics.[22]

In this work, to look for molecules that may donate electrons to FeSe layers, the charge transfer between metal phthalocyanine (*M*Pc, M = Mn, Ni, and Fe) and FeSe monolayer

†Corresponding author. E-mail: sxdu@iphy.ac.cn

© 2025 Chinese Physical Society and IOP Publishing Ltd. All rights, including for text and data mining, AI training, and similar technologies, are reserved.

and that between CoPc (CuPc) and 1–5 layers of FeSe have been investigated using first principle calculations based on density functional theory. The calculation results show that there is an accumulation of electrons at the interface between the MPc molecule and the FeSe layers. The Pc ligand is the primary source of electrons transferred from MPc molecules to FeSe. When integrating the planar charge difference in the z-direction up to the position with zero integrated charge transfer, it is found that electron transfers from CoPc to FeSe with the electron donation increasing as the FeSe layer number increases, converging at 3–5 layers. Meanwhile, CuPc/FeSe shows similar electron transfer as the FeSe layer number increases. All the five MPc molecules contribute electrons to the FeSe substrate, making them promising candidates for tuning the superconducting transition temperature of FeSe systems.

2. Theoretical method

Density functional theory (DFT) calculations were performed using the Vienna *Ab Initio* Simulation Package (VASP),[23] leveraging the projector augmented-wave (PAW) method[22] for the treatment of core electrons. The Perdew–Burke–Ernzerhof (PBE) formulation of the generalized gradient approximation (GGA)[24] was employed, augmented with van der Waals density functionals (vdW-DF)[25] to better represent nonlocal correlations and cohesive effects. The vdW corrected DFT method (vdW–DF/optB86b) is notably prevalent in the computational examination of molecular adsorption on metal surfaces.[26] The kinetic energy cutoff of plane-wave basis set is 450 eV. The force convergence criterion is 0.01 eV/Å. The magnetic configurations of both MPc molecules and Fe atoms in the FeSe layer were taken into consideration. DFT $+U$ was used to address the magnetism of the magnetic MPc molecules. The U value of 4.0 eV and J value of 1.0 eV were applied to the metal atoms.

The differential charge density between the free molecule and its adsorbed configuration on the substrate is quantified using the equation

$$\Delta\rho_{\mathrm{MPc/FeSe}} = \rho_{\mathrm{MPc/FeSe}} - \rho_{\mathrm{MPc}} - \rho_{\mathrm{FeSe}}, \tag{1}$$

where $\rho_{\mathrm{MPc/FeSe}}$, ρ_{MPc} and ρ_{FeSe} denote the electron densities of the adsorption system, the isolated MPc molecule in vacuum, and the freestanding multilayer FeSe, respectively.

3. Electron doping in CoPc/FeSe and CuPc/FeSe systems

Using CoPc and CuPc as examples, we calculated the charge rearrangement in MPc/FeSe systems, with the system configuration illustrated in Fig. 1. To model the organic molecules adsorbed on FeSe layers, slab models with a vacuum length exceeding 14 Å were employed to avoid interactions between molecules and the bottom layer of the substrate due to the periodicity. The lattice constant of FeSe was set to 3.84 Å, consistent with experimental observations.[27] Subsequently, a superlattice of $\sqrt{13}\times\sqrt{13}$ FeSe was constructed with a superlattice constant of 14.07 Å.

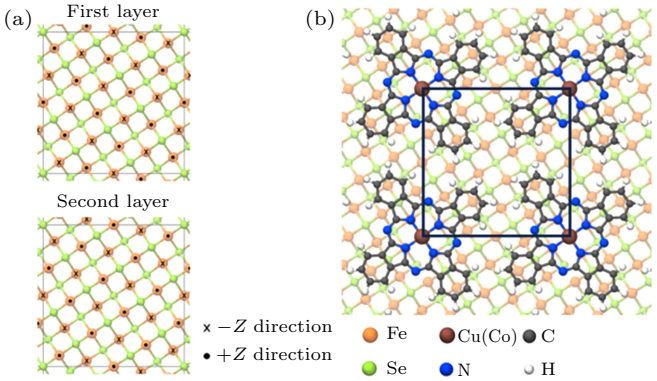


Fig. 1. Illustration of magnetic and adsorption configurations in the FeSe-based system. (a) Magnetic configurations within a bilayer FeSe structure. The dots represent magnetic moments positive along the Z axis, whereas the crosses signify those along the opposite Z direction. (b) Adsorption of a CuPc or a CoPc molecule on a monolayer FeSe. The unit cell is outlined by a black square with a lattice constant of 14.07 Å. Fe, Se, Cu (Co), N, C, and H atoms are in orange, green, brown, blue, dark grey, and white, respectively.

FeSe exhibits $S = 1$ nematic quantum-disordered paramagnet interpolating between the Néel and stripe magnetic instabilities.[28] After evaluation of the Néel and stripe magnetic configurations in monolayer FeSe, the Néel configuration with a lower energy is used for further investigation, with the interlayer magnetic configuration demonstrating an antiparallel orientation, as depicted in Fig. 1(a). CoPc and CuPc molecules were adsorbed onto the FeSe layer, with the metal atoms (Co or Cu) centered above the Se atoms and their D4 symmetry axes aligned parallel to the z-direction (Fig. 1(b)). To verify the stability of this configuration, we compared the total energies of different possible adsorption configurations, including Fe-top, hollow-top, Se-top, and Se-top with a rotation angle (θ°). The lowest total energy confirms that the Se-top configuration (Fig. 1(b)) is the most stable one. Details of these configurations and their relative total energy distributions are provided in Fig. S4 and Table S2, respectively. The Se-top adsorption configuration has a net magnetic moment of 1 μ_{B} along the z-direction.

To investigate the influence of the molecule adsorption on the FeSe layer, the Co(Cu)Pc/FeSe systems with the FeSe layer varying from monolayer up to five layers were examined. The left panels in Fig. 2 represent the charge density difference of the CoPc-adsorbed FeSe layers system, suggesting that electrons accumulate at the interface between the CoPc molecule and the FeSe layer.

The charge rearrangement is predominantly localized within the CoPc molecule and the uppermost FeSe layer. Specifically, charge depletion occurs mainly on the Pc ligand of CoPc (Fig. S1), while charge accumulation is primarily observed at the interface. To further analyze the electron accumulation between CoPc and the FeSe layers, we integrated the planar differential charge along the z-direction (right panels in Fig. 2) from the bottom of the FeSe substrate to the position with zero integrated planar charge difference close to the CoPc molecule in the CoPc/FeSe interface. The integration endpoint for quantifying the electron donation between CoPc and the FeSe layers was set at the blue dashed line, which corresponds to the position with zero integrated charge transfer. The integrated results are summarized in Table S1, illustrating that the electron transfers from the CoPc molecule to the uppermost FeSe layer. As the FeSe layer thickness increases, the Pc ligand primarily exhibits charge depletion characteristic, while the transferred charges are predominantly localized at the CoPc/FeSe interface. Notably, the region around the Co atom displays a distinct pattern of charge accumulation-depletion-accumulation along the z direction, reflecting the interfacial charge redistribution behavior. Meanwhile, the electron donation shows an increasing trend, and tends to converge for substrates with 3–5 layers, indicating that electron donation reaches a saturation point when the FeSe layer thickness exceeds three layers (Table S1).

To further explore the electron doping behavior in different molecular adsorption systems, we also investigated CuPc/FeSe. Similar to the CoPc/FeSe system, the charge density difference of the CuPc/FeSe systems reveals that the electron accumulates at the interface between the CuPc molecule and the FeSe layer (Fig. 3). The integrated planar charge difference in the z-direction, performed up to the position with zero integrated charge transfer, demonstrates that electron transfer from the CuPc molecule to the FeSe layer. In addition, the uppermost FeSe layer captures the majority of electrons donated by the adsorbed CuPc.

In both CoPc/FeSe and CuPc/FeSe systems, electrons predominantly accumulate at the interface. Based on the integration results of the planar charge difference in the z-direction, electrons transfer from the molecule to the uppermost FeSe layer. Since the electron doping is crucial for enhancing superconductivity in FeSe films, the observed electron donation in the two systems suggests that the uppermost FeSe layer may exhibit superconducting properties at certain temperatures (below the superconducting transition temperature (T_c)). A prior research shows that the topmost FeSe layer exhibits enhanced T_c with potassium doping in FeSe thin films regardless of film thickness,[18] indicating the necessity for further experimental investigations for the superconductivity performance of the CoPc/FeSe and CuPc/FeSe systems.

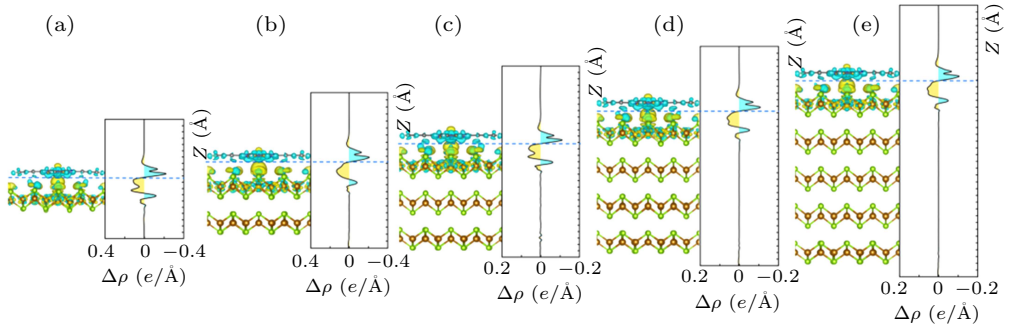


Fig. 2. Charge density differences of the CoPc-adsorbed FeSe layers system. (a)–(e) Left panels: Side views of the charge density difference in CoPc/FeSe systems with monolayer, bilayer, tri-layer, quadri-layer and quintilayer FeSe substrates. The iso-surface is set at ± 0.0002 e/Å^3. Right panels: the corresponding integrated charge densities along the z axis. In these curve panels, yellow regions indicate charge accumulation, while blue regions denote charge depletion, consistent with the color scheme of the charge density difference plots above. The blue dashed line indicates the endpoint for integrating electrons received by the FeSe layers.

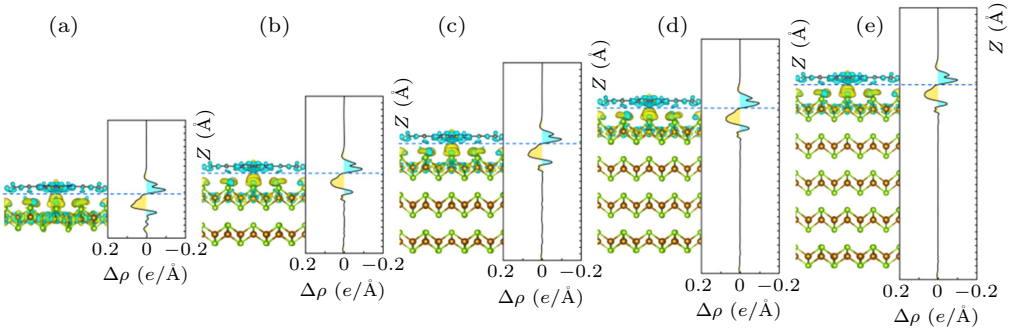


Fig. 3. Charge density differences of the CuPc-adsorbed FeSe layers system. (a)–(e) Left figures: Side views of the charge density difference in CuPc/FeSe systems with monolayer, bilayer, tri-layer, quadri-layer and quintilayer FeSe substrates. The iso-surface is set at ± 0.0002 e/Å^3. Right figures: the corresponding integrated charge densities along the z axis. In these curve panels, yellow regions indicate charge accumulation, while blue regions denote charge depletion, consistent with the color scheme of the charge density difference plots above. The blue dashed line indicates the endpoint for integrating electrons received by the FeSe layers.

4. Electronic structures of CoPc in gas and adsorbed states

Building upon previous charge density difference calculations for the CoPc/FeSe and CuPc/FeSe systems, we further extend our investigation to analyze the electronic structures of CoPc and CuPc in both their gas and adsorbed states. Figure 4(a) presents the projected density of states (PDOS) of CoPc molecules in gas phase, showing the orbital contributions to the electronic states. The molecular orbitals of a gas phase CoPc molecule near the Fermi level are presented in Figs. 4(b)–4(d). Figure 4(b) reveals that the highest occupied molecular orbital (HOMO) exhibits the wave function predominantly localized on the Pc ligand, confirming contributions from p_z orbitals without d-character, which is in accordance with the PDOS results in Fig. 4(a). The lowest unoccupied molecular orbital (LUMO) is mainly contributed by p_z orbitals, with minor contributions from d_{xz} and d_{yz} orbitals. Its wave function primarily localizes on the Pc ligand and only a small portion on the Co atom, as illustrated in Fig. 4(c). In addition, the LUMO+1 corresponds to the $3d_{z^2}$ orbital of the Co atom, as illustrated in Fig. 4(d).

The PDOS of CoPc in CoPc/FeSe is shown in Fig. 4(e). In detail, the HOMO (m_1) retains its spatial distribution as illustrated in Figs. 4(b) and 4(f)). The LUMO (m_2) displays analogous partial charge characters (Fig. 4(g)) to that of the gas phase CoPc (Fig. 4(c)), indicating negligible changes of LUMO of CoPc when adsorbed on FeSe. Notably, the adsorption induces a decrease in the peak height and an increase in the peak width of the LUMO+1 which originates from the out-of-plane d orbitals. From the partial charge density of m_3 (Fig. 4(h)), we observe that m_3 retains a similar configuration as the LUMO+1 of gas phase CoPc but shows a lower density of electron states, suggesting that m_3 is indeed a part of the LUMO+1 in the gas phase. By comparing the PDOS shown in Figs. 4(a) and 4(e), it is found that the electronic states below the HOMO change upon adsorption with peak height decreasing and peak width increasing, indicating the electron rearrangement in the CoPc molecule due to adsorption. These characteristics suggest that electron rearrangement is primarily mediated by the Pc ligand of the CoPc molecule.

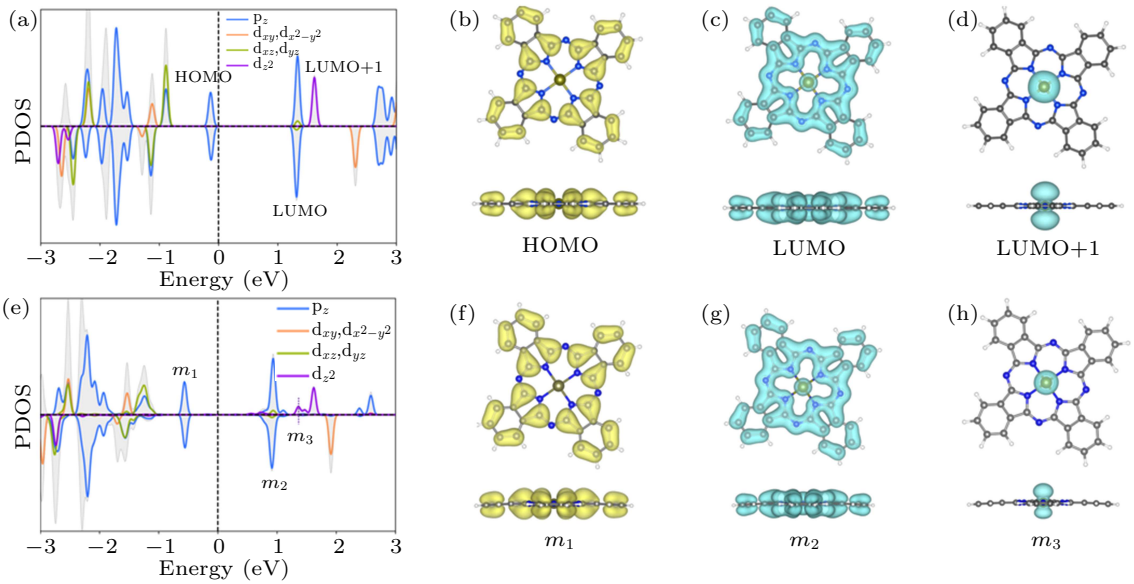


Fig. 4. The PDOS and molecular orbitals of a free-standing CoPc and CoPc on a monolayer FeSe. (a) PDOS for a free-standing CoPc molecule, with the grey area representing the total density of states and lines of various colors depicting different molecular orbitals. (b)–(d) Illustrations of the partial charge density for the HOMO, LUMO, and LUMO+1 orbitals, respectively. The occupied states are highlighted in yellow and unoccupied states in blue, emphasizing the distinction between filled and unfilled states. (e) PDOS attributed to the CoPc molecule in CoPc/FeSe, indicating changes in electronic properties. (f)–(h) Details of the partial charge density of molecular orbitals m_1 (HOMO), m_2 (LUMO), m_3 (HOMO+1), respectively. Each panel presents the partial charge density of the corresponding state, with the top and side views depicted above and below.

Besides the CoPc/FeSe system, the PDOS and partial charge density near the Fermi level for a CuPc molecule in gas phase and adsorbed phase (CuPc/FeSe) were plotted in Fig. S2. Similar to CoPc in CoPc/FeSe, the electronic states below -1 eV change, indicating the electron rearrangement in CuPc molecule. Additionally, MnPc, NiPc, and FePc are further explored to evaluate the electron donation behavior from an MPc molecule to the FeSe layer (Fig. S3). Related calculation results indicate that all the three MPc molecules contribute electrons to the FeSe layer upon adsorption, making them promising candidates for promoting electron accumulation in the FeSe substrate. Detailed discussions are presented in SI. These results call for further experimental explorations into the electron doping mechanisms with FeSe substrate.

5. Conclusion

In conclusion, this work proposed the potential of various metal phthalocyanine (MPc, with M = Co, Cu, Mn, Ni, and Fe) molecules to donate electrons to FeSe layers. The find-

ings reveal the electrons accumulate at the interface between the MPc molecule and the FeSe layer, primarily originating from the Pc ligand. Specifically, CoPc demonstrates increasing electron donation to FeSe as the number of FeSe layers increases when integrating the planar charge density difference up to the position with zero integrated charge transfer, converging at 3–5 layers. CuPc exhibits nearly stable electron transfer with increasing FeSe layer numbers. In addition, MnPc, NiPc, and FePc all contribute electrons to the FeSe layer when adsorbed on monolayer FeSe. These results indicate that all the five MPc molecules emerge as promising candidates for modulating the superconducting properties in FeSe systems.

Acknowledgements

We acknowledge the financial support from the National Natural Science Foundation of China (Grant No. 62488201) and the National Key Research and Development Program of China (Grant No. 2022YFA1204100).

References

[1] Hilse M, Brown F, Roth J, Munyan S and Engel-Herbert R 2024 *J. Mater. Sci.* **59** 2035
[2] Kobayashi T, Nakagawa H, Ogawa H, Nabeshima F and Maeda A 2023 *J. Phys: Condens. Matter* **35** 41LT01
[3] Ge J F, Liu Z L, Liu C, Gao C L, Qian D, Xue Q K, Liu Y and Jia J F 2015 *Nat. Mater.* **14** 285
[4] Jiao X, Dong W, Shi M, Wang H, Ding C, Wei Z, Gong G, Li Y, Li Y, Zuo B, Wang J, Zhang D, Pan M, Wang L and Xue Q K 2024 *Natl. Sci. Rev.* **11** nwad213
[5] Jiang X, Qin M, Wei X, *et al*. 2023 *Nat. Phys.* **19** 365
[6] Liu D, Zhang W, Mou D, *et al*. 2012 *Nat. Commun.* **3** 931
[7] Ouyang X F, Song Z Y and Zhang Y Z 2024 *Supercond. Sci. Technol.* **37** 75015
[8] Yang H, Zhou Y, Miao G, Xu X, Han X, Zhu X X, Guo J, Wu R and Pan X 2023 *Microsc Microanal* **29** 1629
[9] Zhang C, Liu Z, Chen Z, *et al*. 2017 *Nat. Commun.* **8** 14468
[10] Zakeri K, Rau D, Wettstein J, Döttling M, Jandke J, Yang F, Wulfhekel W and Schmalian J 2023 *Phys. Rev. B* **107** 184508
[11] Zhang W, Li Z, Li F, Zhang H, Peng J, Tang C, Wang Q, He K, Chen X, Wang L, Ma X and Xue Q K 2014 *Phys. Rev. B* **89** 060506
[12] He S, He J, Zhang W, *et al*. 2013 *Nat. Mater.* **12** 605
[13] Cheng F J, Zhang Y M, Fan J Q, *et al* 2023 *Chin. Phys. Lett.* **40** 086801
[14] Wang Q Y, Li Z, Zhang W H, *et al*. 2012 *Chin. Phys. Lett.* **29** 037402
[15] Liu X, Liu D, Zhang W, *et al*. 2014 *Nat. Commun.* **5** 5047
[16] Yoshizawa S, Minamitani E, Vijayaraghavan S, Mishra P, Takagi Y, Yokoyama T, Oba H, Nitta J, Sakamoto K, Watanabe S, Nakayama T and Uchihashi T 2017 *Nano Lett.* **17** 2287
[17] Guan J, Liu J, Liu B, Huang X, Zhu Q, Zhu X, Sun J, Meng S, Wang W and Guo J 2017 *Phys. Rev. B* **95** 205405
[18] Song C L, Zhang H M, Zhong Y, Hu X P, Ji S H, Wang L, He K, Ma X C and Xue Q K 2016 *Phys. Rev. Lett.* **116** 157001
[19] Zheng F, Wang L L, Xue Q K and Zhang P 2016 *Phys. Rev. B* **93** 075428
[20] Sagehashi R, Kobayashi T, Uchihashi T and Sakamoto K 2021 *Surf. Sci.* **705** 121777
[21] Sumi N, Yamada Y, Sasaki M, Arafune R, Takagi N, Yoshizawa S and Uchihashi T 2019 *J. Phys. Chem. C* **123** 8951
[22] Uchihashi T, Yoshizawa S, Minamitani E, Watanabe S, Takagi Y and Yokoyama T 2019 *Mol. Syst. Des. Eng.* **4** 511
[23] Kresse G and Furthmüller J 1996 *Comp. Mater. Sci.* **6** 15
[24] Perdew J P, Burke K and Ernzerhof M 1996 *Phys. Rev. Lett.* **77** 3865
[25] Song C L, Wang Y L, Jiang Y P, Li Z, Wang L, He K, Chen X, Ma X C and Xue Q K 2011 *Phys. Rev. B* **84** 020503
[26] Berland K, Cooper V R, Lee K, Schroder E, Thonhauser T, Hyldgaard P and Lundqvist B I 2015 *Rep. Prog. Phys.* **78** 066501
[27] McQueen T M, Huang Q, Ksenofontov V, Felser C, Xu Q, Zandbergen H, Hor Y S, Allred J, Williams A J, Qu D, Checkelsky J, Ong N P and Cava R J 2009 *Phys. Rev. B* **79** 014522
[28] Wang Q, Shen Y, Pan B, Zhang X, Ikeuchi K, Iida K, Christianson A D, Walker H C, Adroja D T, Abdel-Hafiez M, Chen X, Chareev D A, Vasiliev A N and Zhao J 2016 *Nat. Commun.* **7** 12182